THE IMPORTANCE OF SNOW ENTRAINMENT IN AVALANCHE DYNAMICS CALCULATIONS

Betty Sovilla*, Perry Bartelt and Stefan Margreth
Swiss Federal Institute for Snow and Avalanche Research Flüelastrasse, 11, CH-7260 Davos Dorf

ABSTRACT: Numerical models that predict flow velocities and runout distances of extreme avalanche events are used to delimit hazard maps. These models contain many simplifications, one of which concerns snow entrainment. Most avalanche dynamics models assume that avalanche mass is constant along the track, meaning that no entrainment takes place. This assumption is in clear contradiction to post-event observations of avalanche paths which show that much of the snow cover has been entrained into the avalanche and that deposits are left along the avalanche path.
The primary aim of this work is to show the influence of mass variations on avalanche simulations used for hazard mapping. Suggestions are given to improve hazard mapping procedures.
To verify the influence of entrainment in practical calculations, extreme avalanches from the Winter 1998/99 were back-calculated using the Swiss Guidelines procedures and a new theory considering entrainment. It is shown that if entrainment is neglected, the mass and energy balance of the event is in error. Inclusion of entrainment leads to: (1) a better prediction of runout distances, (2) a more accurate determination of flow and deposition depths and (3) a better control over model parameters.
A simple rule for practical calculations that can help to define the correct avalanche mass is suggested.

Keywords: avalanche dynamics, avalanche mass balance, entrainment, deposition, numerical modelling.

1. INTRODUCTION

Entrainment in snow avalanches has been studied at different experimental sites. The mass balance of sixteen well documented avalanche events occurring at the Vallée de la Sionne (Ammann, 1999) and Pizzac (Sommavilla and Sovilla, 1998) sites has been determined (Sovilla, 2004). This data has been supplemented by studying many of the catastrophic avalanches that occurred in Switzerland during the winter 1998-99 (Gruber and Bartelt, 2000). The analysis of all of these data shows that, on average, avalanches increase their original fracture mass by a factor four (Sovilla, 2004).
These recent investigations are not the only measurements that support the idea that entrainment processes are essential to understand the evolution and destructive power of snow avalanches.

In Russia, for example, systematic investigations of avalanche release and avalanche deposition masses confirmed that avalanches could entrain enormous quantities of snow along the avalanche track (Bozhinskiy A.N., 2000, personal communication). Unfortunately, these measurements were not published, neither were detailed observations along the avalanche path or investigations of the physical forces responsible for erosion. At Ryggfonn, Norway, mass balance was roughly estimated for 12 avalanches: It was found that in average, avalanches double their mass from release to deposition (Issler, 2003, personal communication).

In order to understand how the entrained mass influences the energy balance, photogrammetric measurements made at the Vallée de la Sionne test site (Vallet et al., 2001; Sovilla, 2004) were used to approximate the potential energy of seven of the measured avalanche events (see Figure 1). The potential energy of the release mass P_r is compared to the potential energy of the entrained snow P_e. The potential energy was defined from the reference datum, which in this case is the elevation of the beginning of the runout zone. There are only two avalanche events where $P_r > P_e$ .For these two events earlier avalanches entrained the snow cover, clearing the track. However, the usual case is that the entrainment potential energy is slightly larger than the release potential energy. The figure shows that neglecting the entrainment mass results in a significant (factor 2) error in the energy

---

* *Corresponding author address:* Betty Sovilla, Swiss Federal Institute for Snow and Avalanche Research Flüelastrasse, 11, CH-7260 Davos Dorf; tel: +41-81-417 02 63; fax: +41-81-417 01 10; email: sovilla@slf.ch.

balance of the avalanche. Thus, if the avalanche has the possibility to entrain mass, i.e. there are favourable snow conditions and a large potential entrainment area (Sovilla, 2004), the role of the initial conditions (release mass) becomes less important than previously assumed.

Despite these field observations present-day numerical models (Salm et al., 1990; SLF, 1999, Bartelt et al., 1999), used to delimit avalanche hazard maps, neglect entrainment. The avalanche mass is assumed to remain constant along the path. (The mass of the avalanche is based on the estimation of the size of the fracture slab.) Although these models are based on momentum and mass conservation equations, they are nonetheless limited because entrainment is not included. The field data also question any effort to calibrate friction coefficients using the release mass and runout distance alone, since the energy balance is significantly influenced by entrainment.

Models can certainly include entrainment; however, difficulties remain: the introduction of entrainment in the models requires additional parameters such as snow cover depth d_e and distribution along the track, which will certainly complicate practical calculations.

The goal of this paper is to identify and discuss the difficulties and advantages of including entrainment in practical avalanche dynamics calculations. A primary requirement is that model accuracy improves with the addition of an important physical process. Moreover, the model parameter space should, in the end, be better defined.

2. ENTRAINMENT INDICES

The Swiss Guidelines (SLF, 1999) contain procedures to calculate the release mass of extreme avalanches. In the following we compare the predictions of the Swiss Guidelines with real avalanches observed at the Vallée de la Sionne test site. In order to estimate the mass error, values (release volumes, mass, etc) calculated using the Swiss Guidelines are denoted using the subscript *SG*, i.e. $A_{rSG,}$ refers the release area calculated according to the Guidelines, whereas A_r refers to the observed release area.

According to the Swiss Guidelines, practitioners calculate the release mass according to:

$M_{rSG}=A_{rSG}\, d_{0SG}\, \rho_{0SG}$

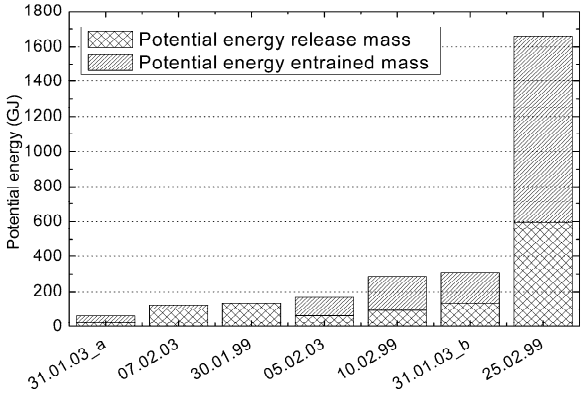

Figure 1. Vallée de la Sionne avalanches. Potential energy of the released and entrained masses at the beginning of the runout zone.

where the release area A_{rSG} is defined by the area in the release zone having a slope angle larger than 30° for a maximum length of 500m (SLF, 1999); the fracture depth d_{0SG} is statistically determined from snow precipitation data and refers to an extreme return period of 300 years and the release density ρ_{SG} is 300 kgm^{-3} (Salm et al., 1990).

The observed avalanche mass is given by the sum of release mass M_r and entrained mass M_e. The release mass is calculated according to:

$$M_r = A_r\, d_0\, \rho_0.$$

where the area A_r, the fracture depth d_0 and the release density ρ (in average 200 kgm^{-3}) are computed from photogrammetry (Vallet et al., 2001), geo-referenced aerial pictures or field measurements (Sovilla et al., 2001).

The entrained mass M_e is defined as the difference between the deposited and released masses:

$$M_e=M_d-M_r$$

The deposited mass M_d is measured after the event using photogrammetry.

The average entrainment depth is defined as:

$$de = \frac{M_e}{\rho_e \cdot A_e}$$

where ρ_e is the density of the entrained snow and A_e is the potential entrainment area, i.e. the area affected by the avalanche passage, excluding the release area A_r .

To facilitate the comparison between

observations and the procedures used in the Guidelines indices are introduced: the growth index

$I_g = M_d / M_r$

quantifies the avalanche mass increase due to snow entrainment; the potential entrainment index

$I_{pe} = A_e / A_r$

is an indicator of the possible mass increase and the entrainment index

$I_e = d_e / d_0$

provides a relation between the release fracture depth and the entrainment depth. Similar indices can also be defined using the Swiss Guideline values, as shown in Table 1.

During the Winter seasons from 1997 to 2003, the mass balance of sixteen avalanches were determined (Sovilla, 2004). However, only six of these avalanches are used in the analysis, because they can be considered as catastrophic. The guideline procedures refer only to avalanches having large return periods (300 years).

Figure 2 shows the indices of the measurements collected during the extreme Winter 1999, in Switzerland.

Table 1. Indices and general definitions.

Definition	Observed	Swiss Guidelines
Release area	A_r	A_{rSG}
Potential entr. area	A_e	A_{eSG}
Fracture depth	d_0	d_{0SG}
Release mass	M_r	M_{rSG}
Deposit mass	M_d	M_d
Entrainment depth	$d_e = \frac{M_d - M_r}{A_e \cdot \rho_e}$	$d_{eSG} = \frac{M_d - M_{rSG}}{A_{eSG} \cdot 300}$
Growth index	$I_g = \frac{M_d}{M_r}$	$I_{gSG} = \frac{M_d}{M_{rSG}}$
Potential entrainment index	$I_{pe} = \frac{A_e}{A_r}$	$I_{peSG} = \frac{A_{eSG}}{A_{rSG}}$
Entrainment index	$I_e = \frac{d_e}{d_0}$	$I_{eSG} = \frac{d_{eSG}}{d_{0SG}}$

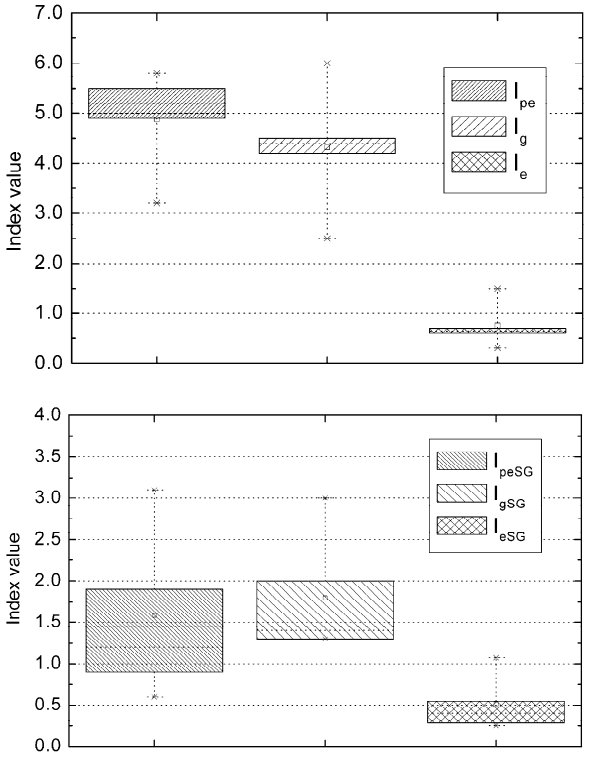

Figure 2. Observed (upper panel) and Swiss Guideline (bottom panel) potential erosion I_{pe}, growth I_g and entrainment I_e indices. Box plots show the mean (square in box), median (line in box), 25/75% quantiles (box), 5/95% quantiles (whiskers) and 0/100% quantiles (cross).

The potential erosion I_{pe}, growth I_g and entrainment I_e indices for both observations and Swiss Guideline procedures (suffix SG) are plotted. Avalanches were characterized by a potential entrainment index I_{pe} between 3.2 and 5.8. The large potential entrainment areas allowed avalanches to increase their mass substantially by entrainment. On average, avalanches increased their mass by a factor $I_g = 4.3$; a maximum value of $I_g = 6$ was measured.

Entrainment is, of course, related to the amount of erodable snow along the avalanche path. On average avalanches entrained a snow depth $d_e = 0.75\ d_0$. The entrainment index I_e varied significantly ($0.3 < I_e < 1.5$).

Indices calculated using the Swiss Guidelines procedures differ considerably from the values based on observations. The release area as defined in the guidelines A_{rSG} is always larger than the observed release area A_r. The potential entrainment index decreases to an average value of 1.6; the average growth index decrease to 1.8,

with a maximum value of 3 and the entrainment depth d_e = 0.50 d_0.

This result is due to the Guideline overestimation of the avalanche release area.

Thus, when entrainment is not considered in practical applications, the mass error is partially corrected by defining a larger release mass. Note, however, that even by increasing the dimensions of the release area, the avalanche mass is still underestimated by 80% (I_{gSG}=1.8) (in average) by a maximum of 200%, which is considerable amount.

3. MODELING AVALANCHES WITH ENTRAINMENT

From experimental observations, Sovilla (2004) found that:

- Three mechanisms of erosion are possible: *front entrainment, step entrainment and basal erosion*. However, only the first contributes to a significant increase in avalanche mass. Ploughing or front entrainment occurs when the snow cover is dry, of low density and cohesion less. Entrainment rates are high since and avalanche can entrain this snow easily. Step entrainment can also lead to high entrainment rates; however, the process is less common. It depends on the layered structure of the snow cover. It is commonly observed when the snow cover contains low strength snow layers sandwiched between ice crusts. In step entrainment, the avalanche breaks the crust layer and instantaneously entrains the underlying snow cover. Analogous to the ploughing case, a large amount of snow can suddenly enter the avalanche. The location is no longer directly at the front, however. Basal erosion is the third possible mechanism. Entrainment rates due to this process are low (Sovilla, 2004). Subsequently, this entrainment process will not be considered further.
- Topography such as slope and path characteristics (canalized, open slope) are not the most important cause for entrainment; it was observed that avalanches following the same path can have completely different growth indices.
- Observations show only a weak correlation between erosion and flow velocity and pressure of the avalanches (Sovilla et al., submitted paper). Both small and large avalanches entrained the same amount of snow with completely different velocities, leading us to believe that entrainment rates are related only to the *amount* of erodable snow along the avalanche path.

These observations confirm that the depth and structure of the snow cover (new snow layers, ice crusts) are more important than topographic features (slope angle, surface roughness) or dynamical characteristics of the avalanche (velocity, pressure) to describe entrainment.

In summary, entrainment is a mass controlled and not a rate controlled process. An entrainment model must therefore determine *how much* and not how fast snow is entrained. A model that simulates immediate uptake is appropriate.

For practical purposes, entrainment can be described by defining an erodable snow cover, i.e. a potential erosion area A_e and an entrainment depth d_e. The modelled avalanche will entrain all the snow cover immediately at the front.

3.1 Model parameterization

The primary weakness of avalanche dynamics models is the uncertainty regarding input parameters (fracture slab height and area). Additional input parameters will certainly be required when the models are extended to include snow entrainment.

A sensitivity analysis of the most common models used in practice (without entrainment) was carried out by Barbolini et al. (2000). The analysis pointed out that the model results, either in terms of runout distance or impact pressure, are remarkably sensitive to friction coefficients and the initial conditions.

We have found that, in addition to the parameters above, model results in simulations where entrainment is considered are additionally influenced by:

- The entrainment depth d_e and
- The ratio between release A_r and entrainment A_e areas. It should be pointed out that in simulations with snow entrainment one has the option of choosing a large release area with a small entrainment area or a small release area and a large entrainment area.

In order to better understand how the entrainment variables affect the model results (velocities, flow depths and runout distances), an example calculation is provided and described below. In a series of simulations we varied the entrainment parameters and noted the subsequent changes in the model results.

To perform this analysis we used a simplified topography composed of two segments having constant slope angle of 35° and 5°, respectively. The avalanche width is constant; the release depth is 1 m and the release density 300 kgm^{-3}.

Calculations were performed with a continuum model (Bartelt et al., 1999), (Norem et al., 1989). The avalanche mass is constant but the snow mass is introduced alternatively as release mass or as entrainment mass varying the ratio A_0/A_e, or alternatively the ratio L_0/L_e since the avalanche width is constant.

In Figure 3 the bold lines represent control calculations where there are no perturbations of the snow cover depth or Coulomb friction coefficient b, which represents the tangent of the internal friction angle of the flowing material. The figure depicts the runout distance *S*, flow depth *h* and velocity *U*, obtained by increasing the release length L_0, which implies a corresponding decrease in the entrainment length L_e (x-axis). Suffix *P* indicates flow depths h_P and velocities U_P calculated at the point *P* located at the change in slope along the avalanche path. Data are made dimensionless by scaling with the runout S_1, flow depth h_{P1} and velocity U_{P1} calculated for the case L_0/L_e = 0.1.

Note that varying the release/entrainment length changes the results significantly. The avalanche flow depths appear to be most sensitive to these changes. Increasing the release length by a factor of five reduces the flow depth by approximately 20%.

The velocity at P and runout distance are reduced by approximately 16% and 7%, respectively. That is, avalanches that entrain mass have longer runout distances.

The reason for this behaviour is that when a large part of the mass is defined as release mass, it is spread out over length of the avalanche. The avalanche depth remains small. In contrast, when the majority of the mass is defined as entrainment the snow accumulates at the front (where it is entrained) resulting in higher flow depths. The entrained snow is not instantaneously spread over the avalanche.

The simulations were then recalculated introducing ±30% perturbations in the friction parameter, the Coulomb friction *b* (Barbolini et al., 2000), on the release depth d_0 and entrainment depth d_e. Changes were always performed individually, i.e. the other parameters were held at their reference values.

Simulations with entrainment show that velocity and runout distance are still sensitive to the variation of the friction parameter *b*, which mainly controls the velocity and runout distance. Variations of approximately 25% for the speed and 19% for the runout were calculated.

Perturbing *b* has little influence on the

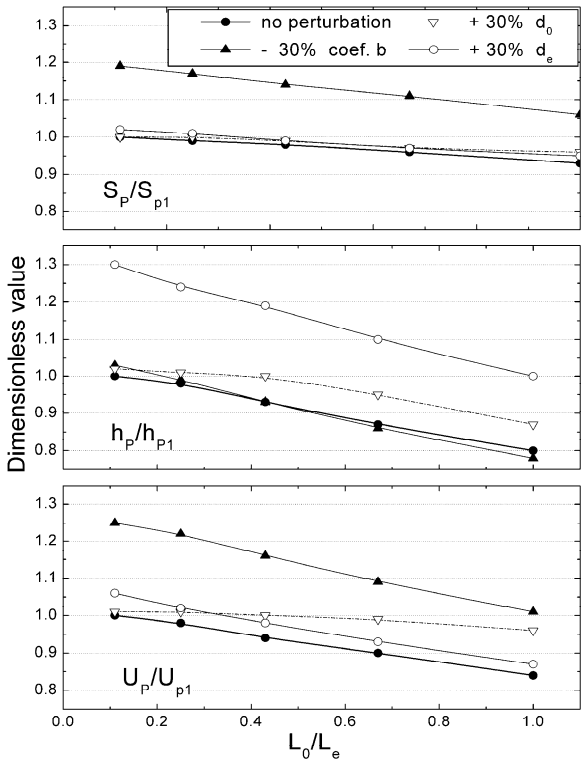

Figure 3. Model sensitivity to changes in release L_0/entrainment L_e length (x-axis) and 30% variations of the friction parameter *b*, release depth d_0 and entrainment depth d_e on runout distance *S*, flow depth *h* and velocity *U*. See text for explanation of U_P, U_{P1}, h_P, h_{P1}, *S* and S_1.

avalanche depth. It is interesting to observe that for avalanches with small release and large entrainment areas (L_0/L_e = 0.1), simulations with entrainment are still remarkably sensitive to the friction parameters (a perturbation of 30% on *b* produced a 19% variation on the runout distance and 25% on the maximum velocity) but are less sensitive to variations of the release depth and area. A perturbation of 30% on d_0 produced a 2-3% variation on the maximum velocity and flow depths and 1% on the runout distance. Similar values were calculated for a perturbation of the release area of 30% (corresponding to the *x*-axis value 1.3).

This sensitivity analysis shows that introducing entrainment, the additional variables complicate the application of the model, as well as the model calibration.

However, there is another effect that should be taken into account: the influence on the friction parameter range when back-calculating known events, i.e. for events where the entrainment

properties are *known*. For this aim, the six extreme avalanches of the winter 1998/99 were back-calculated using a Voellmy-fluid continuum model (Bartelt et al., 1999). To determine the friction parameter range necessary to fit the observed runout, the following calculations were performed:

- Case 1, with entrainment: the avalanche mass in the calculation corresponds to the observed avalanche mass: i.e. release area A_r, measured fracture depth d_0, entrainment depth d_e
- Case 2, without entrainment: the avalanche mass is defined by the procedure defined by the Swiss Guidelines, i.e.: release area A_{rSG}, fracture depth d_{0SG} (SLF, 1999), no entrainment.

In order to match the observed runout distances, the parameter ξ was set to a constant value (ξ = 2500 ms^{-2}) and the parameter μ was varied. The parameter combinations matching the observed runout are shown in Figure 4.

We find that when simulations with entrainment are performed, the μ parameter range *decreases* substantially. In particular, for simulations without entrainment the parameter is sensitive to the type of path and tends to be higher in the case of channelled avalanches (Sovilla, 2004).

In the case with entrainment, there is no evident distinction between the friction parameters for channelled and open slope avalanches. This is due to the effect of entrainment on flow depth. Flow depth calculated without entrainment (see Figure 7) are extremely low and the effect is particularly evident for open slope avalanche where the mass is more spread-out. The unrealistic flow depth difference between open slope and canalized avalanches and the obvious influence on speed must be controlled by different parameters. This deficiency of numerical models can be corrected by inserting realistic and correct entrainment values.

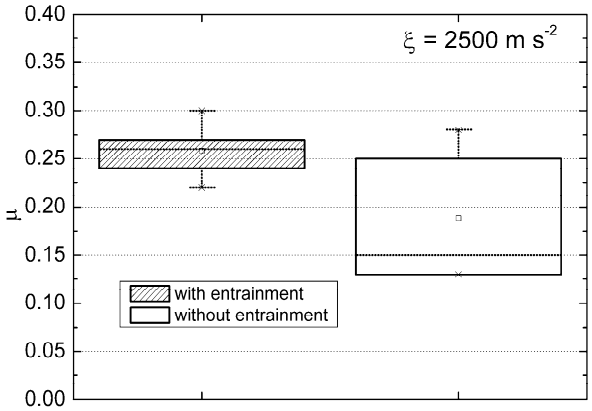

Figure 4. Parameter ranges used to back-calculate the extreme avalanches of 1999. The range of parameter μ in the case of the simulation with entrainment is significantly smaller than the simulation without entrainment. The box plots show the mean (square in box), the median (line in box), 25-75% quantiles (box), 5-95% quantiles (whiskers) and 0-100% quantiles (cross).

In summary, the introduction of entrainment does not necessarily complicate avalanche dynamics calculations. On the contrary, it can help control the parameter range, in particular the all important dry Coloumb friction parameter *b* (or μ).

3.2 Effects of entrainment on model results

To show the effects of introducing entrainment in the flow model on runout distances, flow velocities, pressures and flow heights, avalanche velocities were calculated using the following approaches:

- Without and with entrainment using a continuum depth averaged model (Bartelt et al., 1999) and input parameters as in cases 1 and 2.
- Using the Voellmy-Salm procedure (Salm et al., 1990). The friction parameters for a large avalanche (ξ = 1000 m s^{-2} and μ = *b* = 0.155) were used. The position of the point P is at the intersection of the two segments composing the avalanche path.

The effect on flow velocities is depicted for the two cases in Figure 5. The maximum flow velocities along the avalanche path calculated without and with entrainment are displayed.

On the upper panel calculations are performed using the same parameters for both simulations. It is observed that the avalanche without entrainment increases its speed, reaching a maximum velocity at about the halfway point of the steeper part of the track (x<1000m) and then decelerates. Avalanches entraining snow increase their velocity until they reach the change in slope (x=1000m) where they start to decelerate. The simulation with entrainment reaches the highest maximum speed and longer runout.

On the bottom panel, calculations are performed varying the parameters from case to case to match the runout calculated with the Voellmy-Salm model. To obtain the same runout distance, the parameters used in the simulation without entrainment are lower.

It was also observed that, initially, avalanches that entrain mass have a lower acceleration in

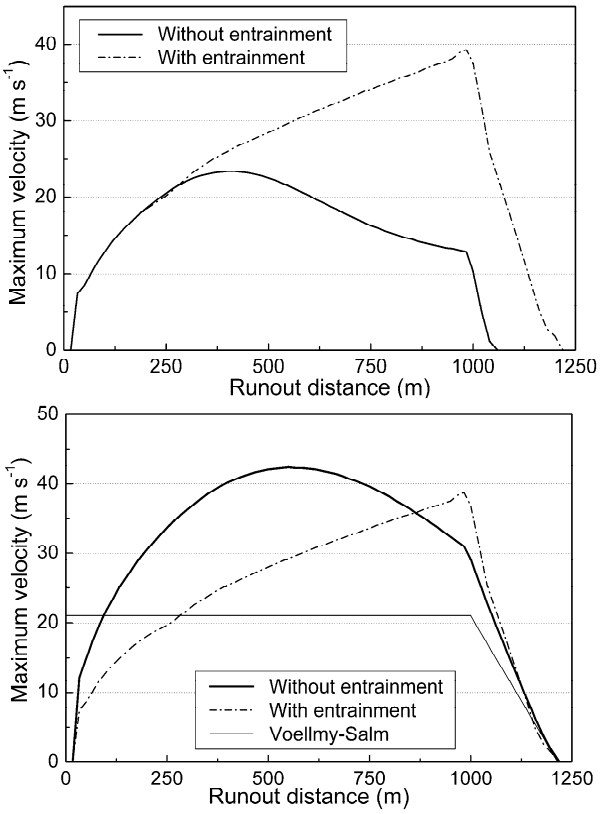

Figure 5. Maximum velocity along the avalanche path. Comparison between simulations without and with entrainment. On the upper panel simulations are performed using the same parameters for both simulations with and without entrainment. On the bottom panel, calculations are performed varying the parameters from case to case to match the runout calculated with the Voellmy-Salm model.

comparison to avalanches that do not entrain snow. This behaviour is explained by the fact that the entrained mass must be accelerated to the avalanche speed, decelerating the avalanche.

However, when the entrainment significantly increases avalanche mass and flow depths, the loss in velocity is offset by reduction of the resistance force. Consequently the typical velocity for an avalanche with entrainment is lower in the first part of the track and higher in the second part. In this particular case, the avalanche with mass variation increases slowly its speed but finally overcomes the velocity of the avalanche without entrainment just before *P*. Note that if the path were shorter, the avalanche with entrainment would not necessarily reach the highest speed.

Effects on pressure can be observed in Figure 6 where the dimensionless ratio U^2/U_P^2 (proportional to the pressure) is plotted as a function of the runout distance. The velocity U_P is the avalanche speed at the point P calculated using the Voellmy-Salm model. The straight bold line represents the results of the Voellmy-Salm model. The other curves display the calculations performed using a continuum model with and without entrainment. We note that at the point *P*, the square of the runout velocity, calculated using the continuum model with entrainment, is considerably higher; however, it decreases below the Voellmy-Salm curve in the second part of the runout as a result of a faster avalanche deceleration.

However the larger effects are on flow depths (see Figure 7); maximum flow depths increase substantially when considering entrainment; entrainment can easily more than double the calculated flow height. Flow heights in simulation models are generally too small and cannot be matched with field observations (Bartelt et al., 1999).

4. SUGGESTIONS FOR THE PRACTICE

The six avalanches of the catastrophic Winter 1998/99 have been calculated following the Swiss Guidelines, i.e. defining both mass and flow parameters as described in SLF, 1999. For three of the six examined avalanches, calculated runout distances were too short. This occurred when the ratio between real and calculation masses M_d/M_{rSG} was larger than 1.35. Figure 8, upper panel shows an example of underestimation of runout.

The corresponding deposition depths are shown in the lower panel.

The comparison between calculated deposition depths and maximum measured deposition depths shows that snow deposition depths reach a realistic value only in the simulations with

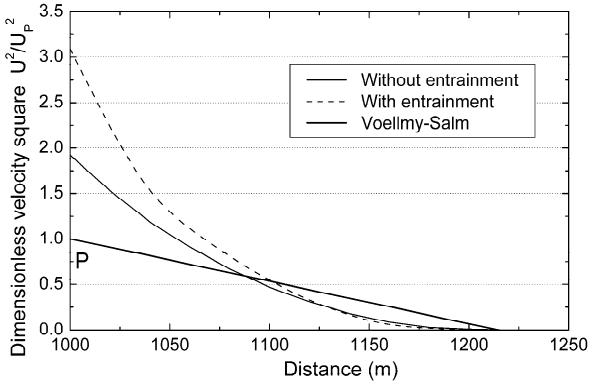

Figure 6. The dimensionless ratio U^2/U_P^2 is plotted as a function of the distance.

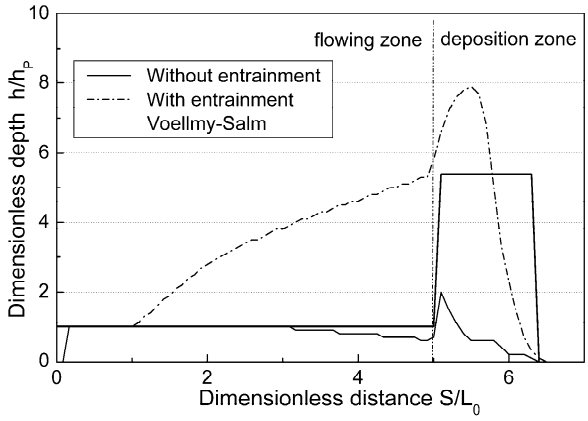

Figure 7. Dimensionless maximum avalanche depth plotted as a function of the dimensionless projected distance.

entrainment. However, there is still a difference between the average deposition depth calculated with the model and the real maximum deposition depths measured in the field, mainly due at the application of a 1D-model to a 3D-phenomena.

Thus, to improve calculations, it is necessary to appropriately choose the avalanche mass. This could be alternatively made by (1) extending the release beyond 500 m on slope angles smaller than 30° or (2) use a model with entrainment defining an erodable snow cover. The second solution is obviously more realistic and is the one that yielded the best results. However, a problem exists: in spite of the fact that models with entrainment are the future of practical calculations, at the moment there are not enough experimental data to calibrate them thoroughly.

It is nonetheless possible to control the error in the definition of the avalanche mass: a suggestion, based on the practice index analysis, is to calculate the avalanche mass M as the sum of released mass M_{rSG} and entrained mass M_e on the basis of the following relation:

$$M = M_{rSG} + M_e = A_{rSG}\, d_{0SG}\, \rho_0 + A_{eSG} d_{eSG}\, \rho_e$$

where $\rho_0 = \rho_e = 300$ kg m^{-3} and $d_{eSG} = 0.5\, d_{0SG}$ which is the average entrainment depth measured for six extreme avalanches of the Winter 1998/99 as shown in Figure 2. The value calculated with the relation above can than be compared with the mass defined by the Guidelines to evaluate the mass error.

5. CONCLUSIONS

At present, entrainment is not considered in practical avalanche dynamics calculations. In this

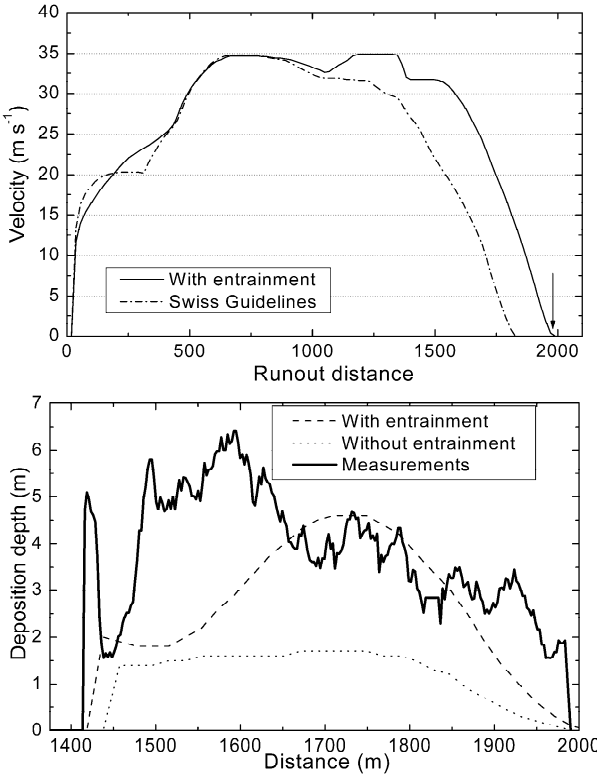

Figure 8. Cheer avalanche. Upper panel: velocity. Lower panel: deposition depths. Simulations are performed using the Swiss Guidelines and with entrainment. On the lower panel deposition depths are compared to maximum depths measured in the field.

work it has been shown that if the calculation mass is underestimated for more than 30%, calculated runout distances can be too.

Flow and deposition depths are underestimated with important negative consequences on avalanche hazard mapping and defence structure dimensioning.

Entrainment can be easily introduced into dynamical calculations since it is governed by few and well defined parameters and in addition, the introduction of entrainment decreases the friction parameter range, making it easier to choose them reasonably.

However, even if entrainment can improve the accuracy of the calculations, the fact remains that model calibration for practical applications requires much experimental data on extreme avalanches. The data actually collected are a unique and important contribution to the field of snow avalanche dynamics and they can be used to define basic guidelines to control errors in avalanche mapping procedures. Additional and extended information for more events is needed to

calibrate entrainment models.

Given the evidence for the importance of the phenomenon presented, avalanche dynamics research can no longer ignore entrainment and deposition processes. In future, research must focus on developing experimental techniques and theoretical models to gain deeper understanding of this phenomenon. However, the results of this work show that even a simple entrainment model can lead to significant improvements in practical hazard mapping calculations.

6. .ACKNOWLEDGEMENTS

Funding for this research has been provided by the Swiss National Foundation. The authors would like to thank the avalanche dynamic team and logistics staff of the SLF for their support in both the field and laboratory experiments.

7. REFERENCES

Ammann, W.J. 1999. A new Swiss test-site for avalanche experiments in the Vallée the la Sionne/Valais. Cold Regions Science and Technology, 30, 3-11.

Bartelt, P., B. Salm and U. Gruber. 1999. Calculating dense-snow avalanche runout using a Voellmy-fluid model with active/passive longitudinal straining. J. Glaciol., 45, 242-254.

Barbolini, M., Gruber U., Keylock C., Naaim M., & Savi F. 2000. Application of statistical and hydraulic continuum dense snow avalanche to five real European sites. Cold Reg. Sci. Technol. 31, 133-149.

Gruber, U. and P. Bartelt. 2000. Study of the 1999 avalanches in the Obergoms valley, Switzerland, with respect to avalanche hazard mapping. Proceeding of the International Snow Science Workshop (ISSW), Big Sky, Montana.

Norem, H., F. Irgens and B. Schieldrop. 1989. Simulation of snow-avalanche flow in run-out zones. Ann. Glaciol., 13, 218-225.

Salm, B., A. Burkard and H. Gubler. 1990. Berechnung von Fliesslawinen: eine Anleitung für Praktiker mit Beispielen. Eidg. Inst. Schnee und Lawinenvorsch. Mitt. 47.

SLF, 1999. Neue Berechnungsmethoden in den Lawinengefahrenkartierung. Davos, Switzerland: Eidg. Inst. Schnee- und Lawinenforschung.

Sommavilla, F. and B. Sovilla. 1998. The avalanche monitoring system of Mount Pizzac. In Hestnes, E., ed. 25 Years of Snow Avalanche Research, Voss, 12-16 May 1998. Proceedings. Oslo, Norwegian Geotechnical Institute, 268-273. (NGI Pubblication 203.)

Sovilla, B. 2004. Field experiments and numerical modelling of mass entrainment and deposition processes in snow avalanches. Ph.D Thesis, ETH Zurich, Switzerland.

Sovilla, B., F. Sommavilla and A. Tomaselli, 2001. Measurements of mass balance in dense snow avalanche events, Ann. Glaciol., 32, 230-236.

Sovilla, B., P. Bartelt and P. Burlando. Submitted paper. Entrainment in snow avalanches.

Vallet, J., U. Gruber and F. Dufour. 2001. Photogrammetric avalanche volume measurements at Vallée de la Sionne. Ann. Glaciol., 32. 141-146.